Electronic Supplementary Material (ESI) for Nanoscale.

Reticular Synthesis of Two-dimensional Ionic Covalent Organic Networks as Metal-free Bifunctional Electrocatalysts for Oxygen Reduction and Evolution Reactions

Pampa Jhariat,[a,b] Arjun Warrier,[b] Ananta Sasmal,[c] Subhadip Das,[d] Shafeeq Sarfudeen,[b] Priyanka Kumari,[b] Arpan Kumar Nayak,[e] and Tamas Panda* [a,b]

Author Information

[a] Centre for Clean Environment, Vellore Institute of Technology, Vellore, Tamil Nadu-632014, India. Email – tamaskumarpanda@vit.ac.in

[b] Department of Chemistry, School of Advanced Sciences, Vellore Institute of Technology, Vellore, Tamil Nadu- 623014, India.

[c] Department of Physics, School of Advanced Sciences, Vellore Institute of Technology, Vellore, Tamil Nadu-623014, India.

[d] Department of chemistry, Chaudhary Ranbir Singh University, Jind, Hariyana-126102, India.

[e] Department of Energy Engineering, Konkuk University, 120 Neungdong-ro, Seoul-05029, Republic of Korea

Page No

S1: General Information

General remarks:

1,1'-bis(2,4-dinitrophenyl)-[4,4'-bipyridine]-1,1'-diium dichloride (L1) was synthesized via previously reported synthetic procedure (S1). N, N'-bis(4-aminophenyl) benzene-1,4-diamine (BPDP) also synthesized according to the previously reported procedure without doing any further modification (S2). All other chemicals were purchased from commercially available source without doing any further purification.

Instruments:

- **Fourier transform infrared (FT-IR) spectra:** Fourier transform infrared (FT-IR) spectra were taken on IRAffinity-1 (Shimadzu, Japan) spectrometer at Zn-Se ATR (attenuated total reflection) mode in the 4000-400 cm^{-1} (mid IR range) region.
- **Powder X-ray diffraction (PXRD):** Bruker D8 Advanced XRD (excitation source: 2.2KW Cu-anode ceramic tube) was used for analysing the PXRD pattern of all the vCONs. We have processed further the PXRD data by using the X'pert High Score Plus software for the background correction.
- **Thermogravimetric analyses (TGA):** Thermo-gravimetric analysis (TGA) was recorded over the temperature range between 25 to 800 °C on a SDT Q600 TG-DTA analyzer in the presence of N_2 atmosphere with heating rate of 20 °C min^{-1}.
- **Gas adsorption:** Adsorption isotherms were measured in Quantachrome USA device at 77 K (maintained by liquid N_2). Before analysis the vCONs samples were degassed for 12h at 100 °C in the presence of liquid nitrogen.
- **Field Emission - Scanning Electron Microscopy (FE-SEM):** The Thermo Fisher FEI QUANTA 250 FEG was used for the FE-SEM analysis the morphological diversity of the four vCONs. The Instrument is equipped with Schottky Field Emission Electron Gun as source of Electrons with operating voltage range 5kV-30kV offering high resolution of 1.2 nm at 30 kV at high vacuum conditions.

- **Nuclear Magnetic Resonance Spectroscopy:** Magic Angle Spinning (MAS) solid-state NMR experiments for vCONs were carried out on a JEOL 400 MHz NMR spectrometer. NMR data were processed using Top-Spin software.

- **Electron Spin Resonance Spectrometer:** Solid state ESR spectra of the radical cation state of four vCONs were measured on JEOL Model JES FA200 spectrometer.

- **Solid state UV-VIS Spectroscopy:** solid state UV-VIS spectra of vCONs were recorded on JASCO (V-670 PC) spectrometer.

- **X-ray photoelectron spectroscopy:** XPS spectra of vCONs were recorded on K-Alpha-KAN9954133 (Thermo Scientific) spectrometer with the monochromatic Al Kα source (Energy range 100-4000 eV) under ultrahigh vacuum (10^{-7} Pa), referenced to the C 1s signal at 284.6 eV .

- **High-Resolution Transmission Electron Microscopy (HR-TEM):** HR-TEM images of vCONs were captured on FEI TECNAI G2 F20 S-TWIN HR(S)TEM microscope.

- **Dynamic Light Scattering (DLS) Particle size analyzer:** particle size analysis of vCONs were carried out on Litesizer 500 (Anton Paar GmbH, Austria)

S-2: Experimental Methodology

S-2.1: Synthesis of vCONs:

The organic linker L1 and corresponding triamines [guanidine chloride (GC), 1,2,3-triaminoguanidine chloride (GAC), melamine (MEL), and N, N´-bis(4-aminophenyl) benzene-1,4-diamine (BPDP)] were used as starting materials to synthesize all vCONs via Zincke's reaction. First, a sealed tube was charged with L-1 (0.5mmol, 0.28g) and respective triamines (0.5 mmol) in 10 mL solution mixture of ethanol and water (4:1 ratio) under the presence of N_2 atmosphere. Then the reaction mixture was degassed through the three freeze-pump-thaw cycles and kept in preheated oven at 120 °C for 72h. After the completion of reaction, the precipitate was collected via centrifugation followed by vacuum filtration and washed with polar solvents like dimethylformamide (DMF), dimethylacetamide (DMAc), ethanol (EtOH), boiling water (H_2O), methanol (MeOH), dichloromethane (DCM), and acetone to remove the small polymers, oligomers and other impurities. After washing, the desired product was kept in a mixture of chloroform and tetrahydrofuran (1: 1) solution [to exchange high boiling solvents with low boiling solvents] for three days. Finally, the product was collected via vacuum filtration and dried over night at 120 °C.

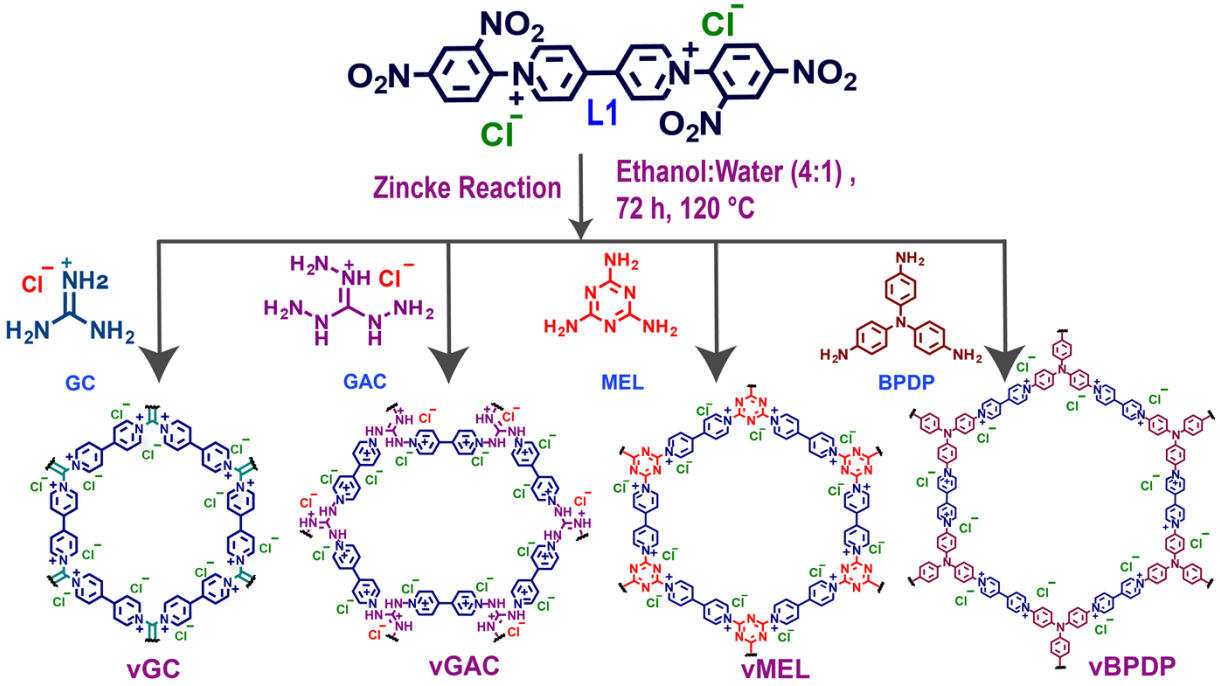

Figure S1: Schematic representation of synthesis of vCONs.

S-2.2: Electrochemical Measurements:

Sample Preparation Method for Electrochemical Measurements:

2 mg of the sample was dispersed in 2 mL of N-methyl 2-pyrrolidone under rigorous sonication for 1 h. Then 1 mL of the resultant ink was re-dispersed in another 4 mL of 2-propanol with 2 drops of Nafion 117 solution (Sigma-Aldrich, USA) under rigorous sonication for 30 min. Thereafter, a total of 20 µL of the resultant slurry was drop-casted by spin-coating method in succession on the 3 mm glassy-carbon disc of the RRDE and was allowed to dry completely at room temperature for more than 24 h. All electrochemical testing were performed using the prepared RRDE at 1000 rpm (unless mentioned otherwise). All observations were recorded in 1.0 M KOH electrolyte. Counter Electrode: Graphite Rod; Reference electrode: Ag/AgCl (satd. KCl).

Determination of Effective Electrochemical Active Surface Area (ECSA):

the electrochemical active surface area (ECSA) was calculated using the double layer capacitance method 1M KOH cyclic voltammetry. Diverse samples in the non-faradaic zone have been subjected to cyclic voltametric (CV) tests with the purpose of calculating the double-layer capacitance (C_{dl}). In a non-faradaic potential zone (0 to 0.1 V vs. Ag/AgCl), cyclic voltammograms were typically obtained at scan speeds of 10, 20, 40, 60, 80, and 100 mV s^{-1}. On this small potential scale, the current can only originate from double-layer charging and discharging rather than charge transfer, as the double-layer current is precisely proportional to the scan rate

$$\mathbf{I = v\ C_{dl}}$$

Therefore, the C_{dl} was determined by plotting the change in current density Δ*J* (anodic current density-cathodic current density) at 0.05 V with various scan rates. Thus, the resultant linear slope is twice the C_{dl}. The ECSA was then determined using the formula

$$\mathbf{ECSA = C_{dl}/C_s}$$

where C_s is the specific capacitance of a material's atomically smooth surface under identical reaction conditions. The roughness factor (R_f) is derived from the ECSA value.

The slopes of these linearly fitted plots was equated to twice of the double-layer capacitance (Cdl) of these materials to evaluate ECSA by the equation:

$$\mathbf{C_{areal} \times ECSA = C_{dl}}$$

where C_{areal} was considered to be 40 µF.cm^{-2} for flat surface. Hence, ECSA (vGAC) = 1.44, ECSA (vGC) = 1.55, ECSA (vBPDP) = 1.51, and ECSA (vMEL) = 1.54.

Koutecky-Levich plot determination:

The slopes and intercepts of Koutecky- Levich plots (J^{-1} *vs.* $\omega^{1/2}$) were evaluated and fitted into the linear curves, where the Koutecky-Levich equation may be used to get the electron transfer number (n) and kinetic current density j_k number:

$$\frac{1}{j} = \frac{1}{j_L} + \frac{1}{j_k} = \frac{1}{B\omega^{1/2}} + \frac{1}{j_k}$$

$$B = 0.62nFC_0(D_0)^{2/3}\nu^{-1/6}$$

$$j_k = nF\kappa C_0$$

where, j = measured current density,

j_k = The kinetic current density.

j_L= The diffusion-limited current density.

ω = The electrode rotation rate.

Electrochemical impedance spectroscopy (EIS) was conducted over a frequency range spanning from 0.01 Hz to 10^6 Hz, employing a 5 mV amplitude. Durability assessments were carried out using chronoamperometry at a potential of 0.40 V (0.1mmol methanol was added at 1000 s.)

S-3: Characterization of vCON

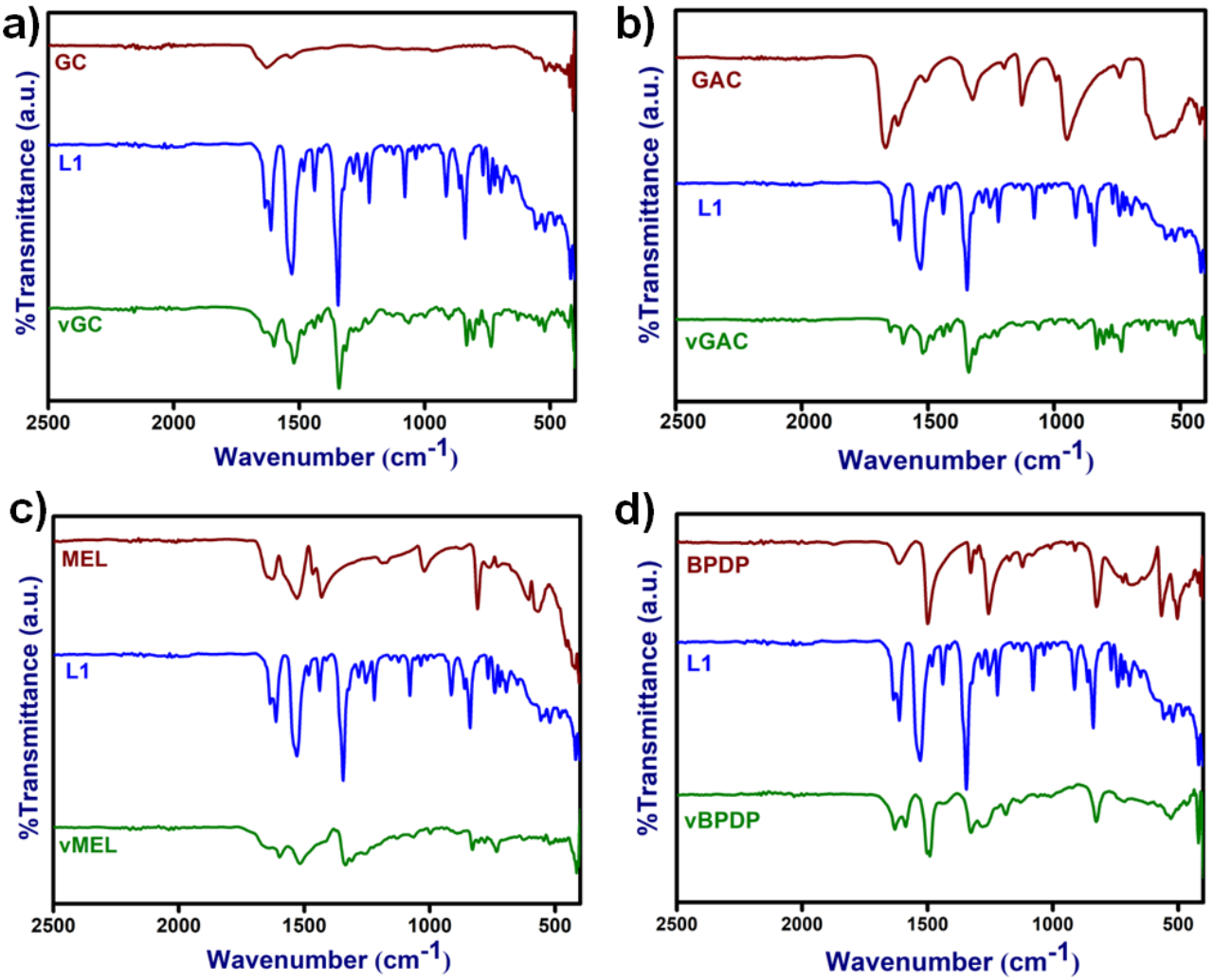

Figure S2: FT-IR spectra of **a)** vGC **b)** vGAC, **c)** vMEL, **d)** vBPDP, compared with their respective starting materials, L1 and respective triamines (GC, GAC, MEL and BPDP). All vCONs are shown by **maroon line**, L1 by **blue line**, and triamines by **olive line**.

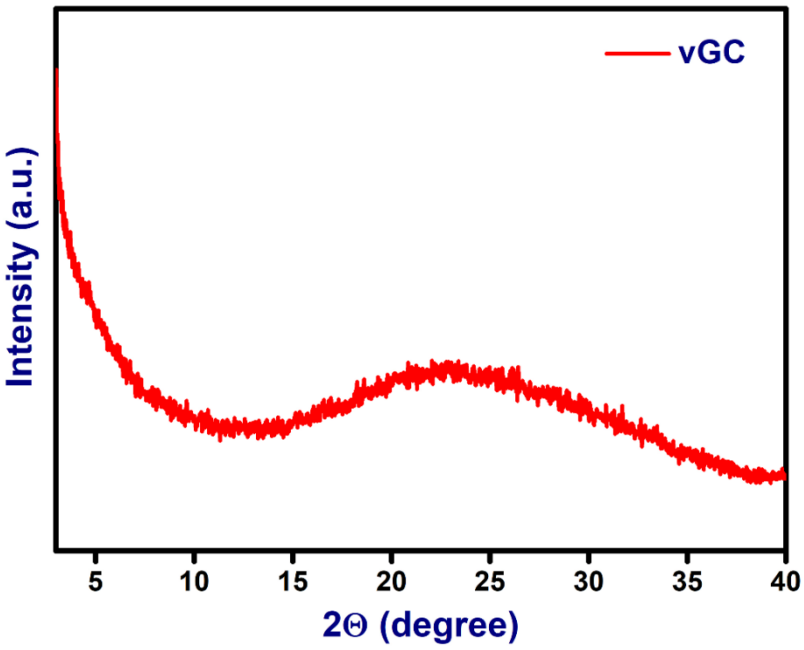

Figure S3: PXRD pattern of as synthesized vGC, which is amorphous in nature

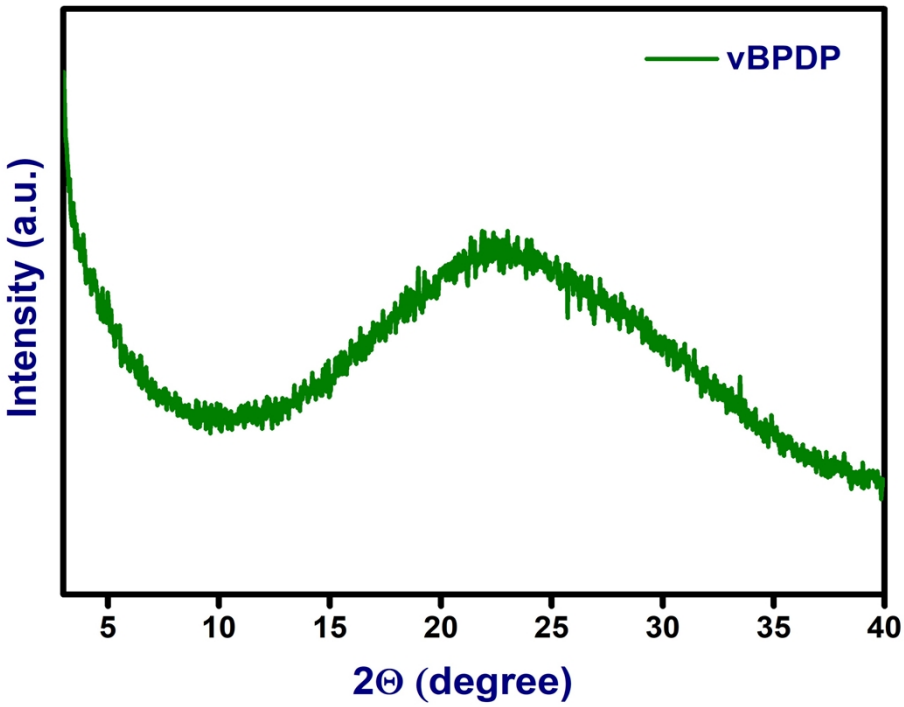

Figure S4: PXRD pattern of as synthesized vBPDP, which is amorphous in nature.

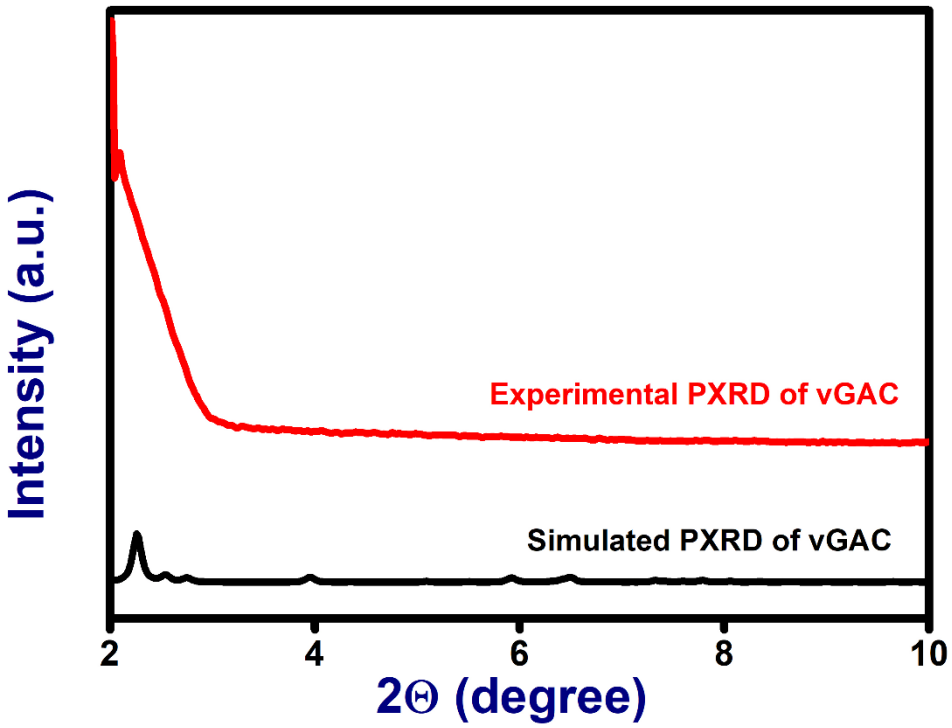

Figure S5: PXRD pattern of as synthesized vGAC (2θ = 2 to 10°).

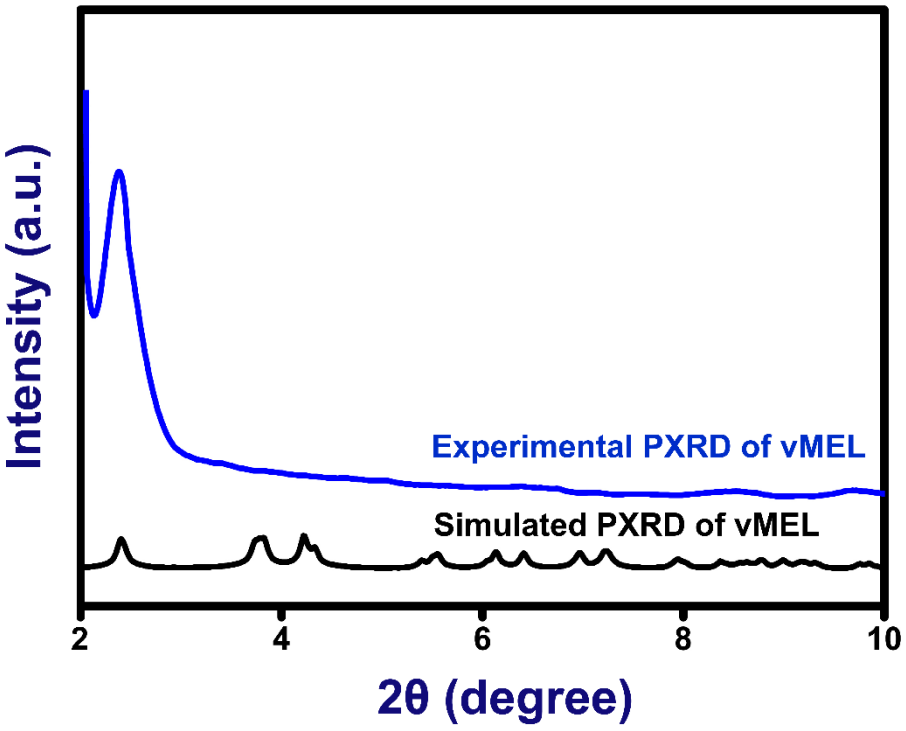

Figure S6: PXRD pattern of as synthesized vMEL(2θ = 2 to 10°).

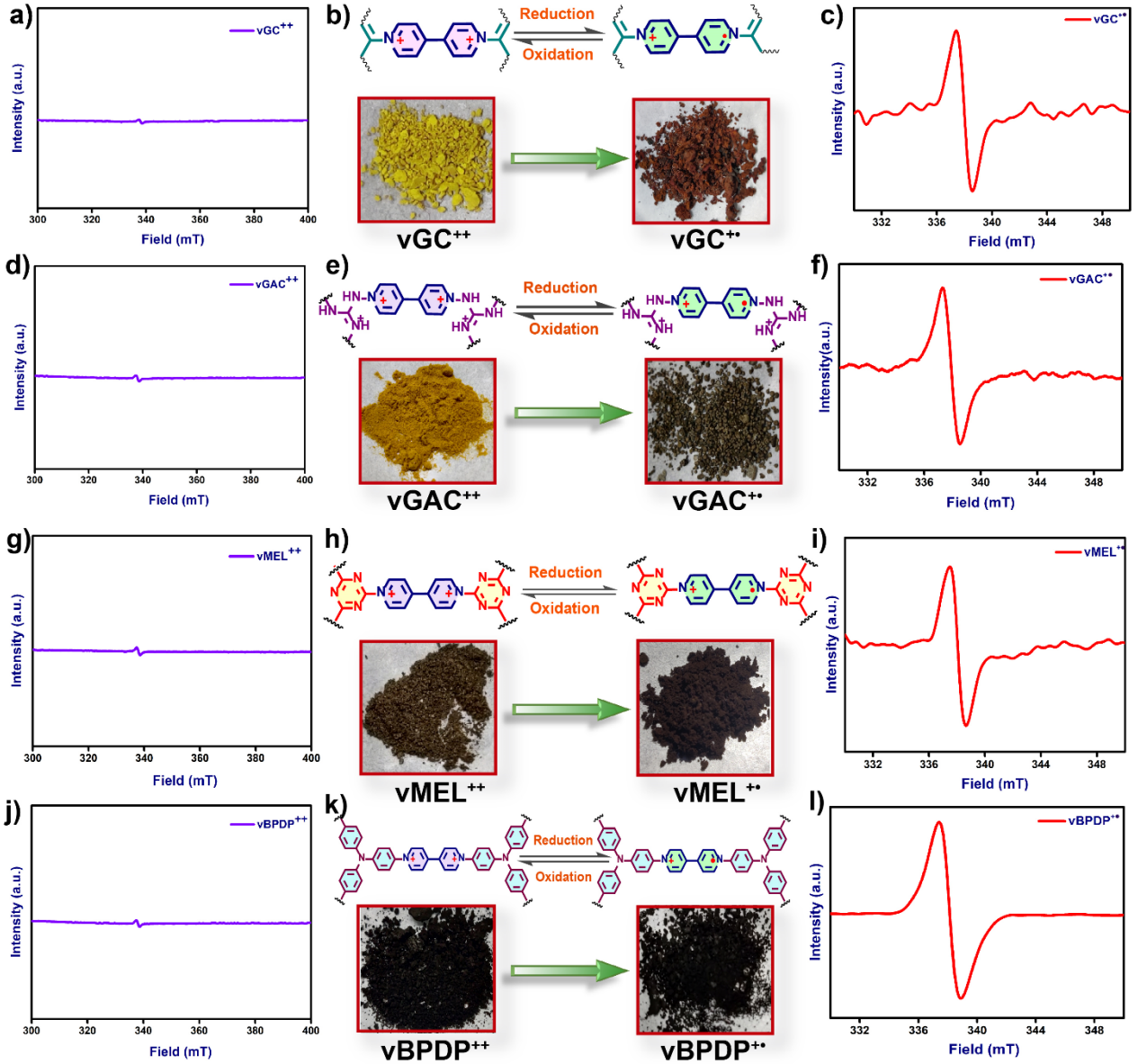

Figure S7: Redox property of the reversible nature of vCONs. **Fig. a, d, g,** and **j** showed the solid state EPR spectra of dicationic vGC, vGAC, vMEL and vBPDP respectively. As there is no unpaired electron in any dicationic vCON, there is no noticeable paramagnetic signal in EPR spectra. **Fig. c, f, i** and **l** showed the solid state EPR spectra of the radical cationic states of vGC, vGAC, vMEL, and vBPDP, respectively. Due to the creation of the radical cationic state of vCONs, a noticeable paramagnetic peak is seen in every instance. **Fig. b, e, h,** and **k** provide a schematic representation of the color change and possible reversible redox nature of vGC, vGAC, vMEL, and vBPDP respectively with real images.

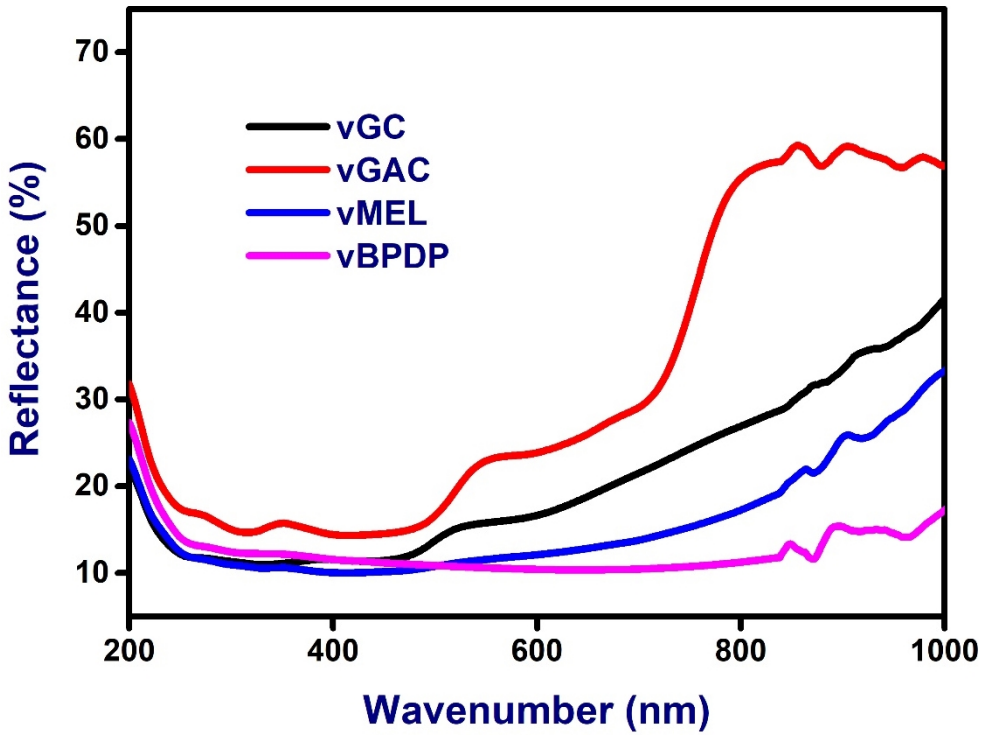

Figure S8: solid state UV-VIS spectra of all vCONs.

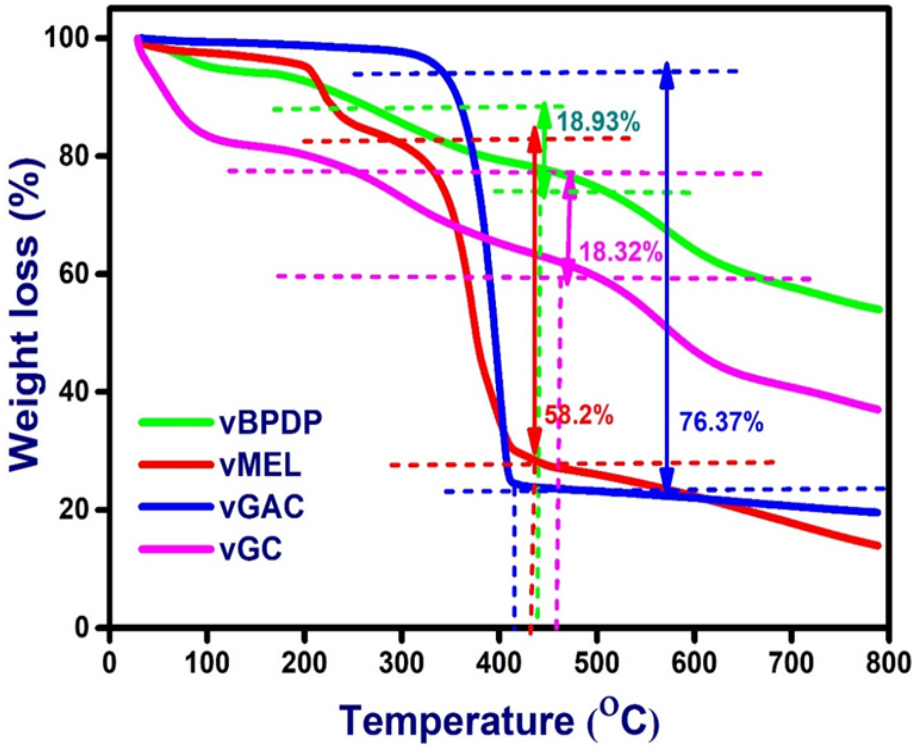

Figure S9: Thermogravimetric analysis (TGA) of all vCONs.

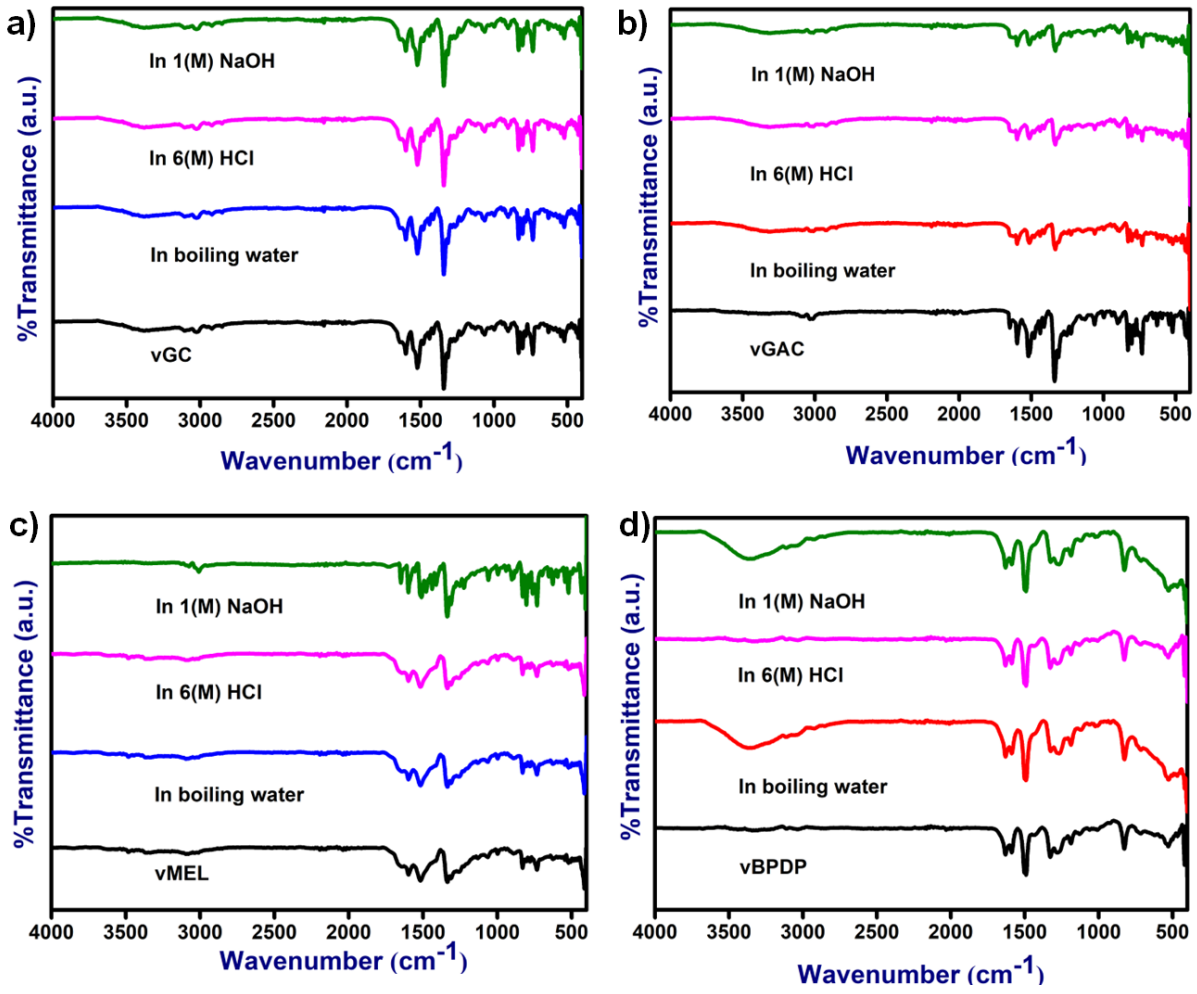

Figure S10: **Chemical stability** of all the vCONs treated. with **1 M NaOH**, **6 M HCl** and **boiling water.** FT-IR spectra of the **1 M NaOH**, **6 M HCl** and **boiling water** treated samples of [a) vGC, b) vGAC , c) vMEL, and d) vBPDP compared with their respective pristine phase.

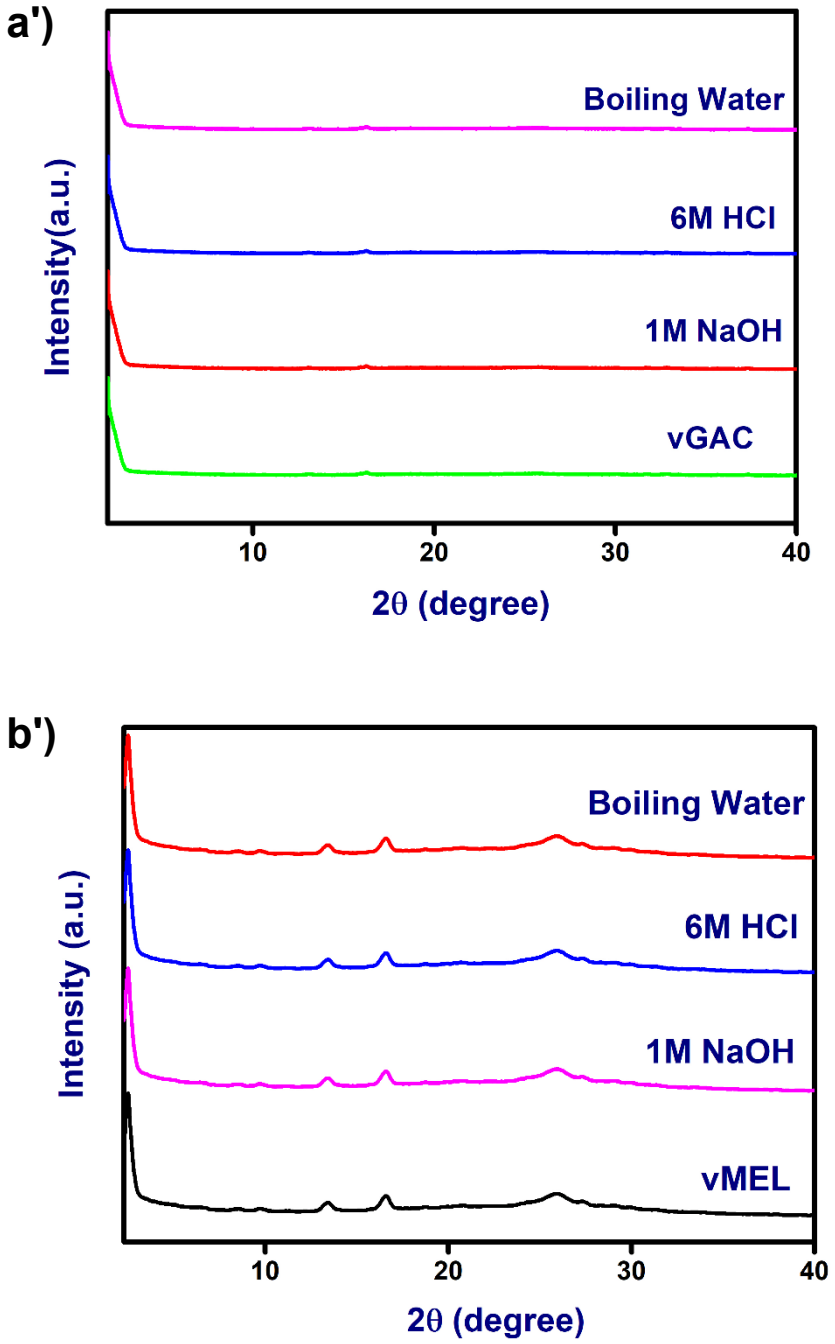

Figure S10: **Chemical stability** of all the vGAC and vMEL treated. with **1 M NaOH**, **6 M HCl,** and **boiling water.** PXRD pattern of the **1 M NaOH**, **6 M HCl,** and **boiling water** treated samples of a') vGAC, and **b')** vMEL, compared with their respective pristine phase.

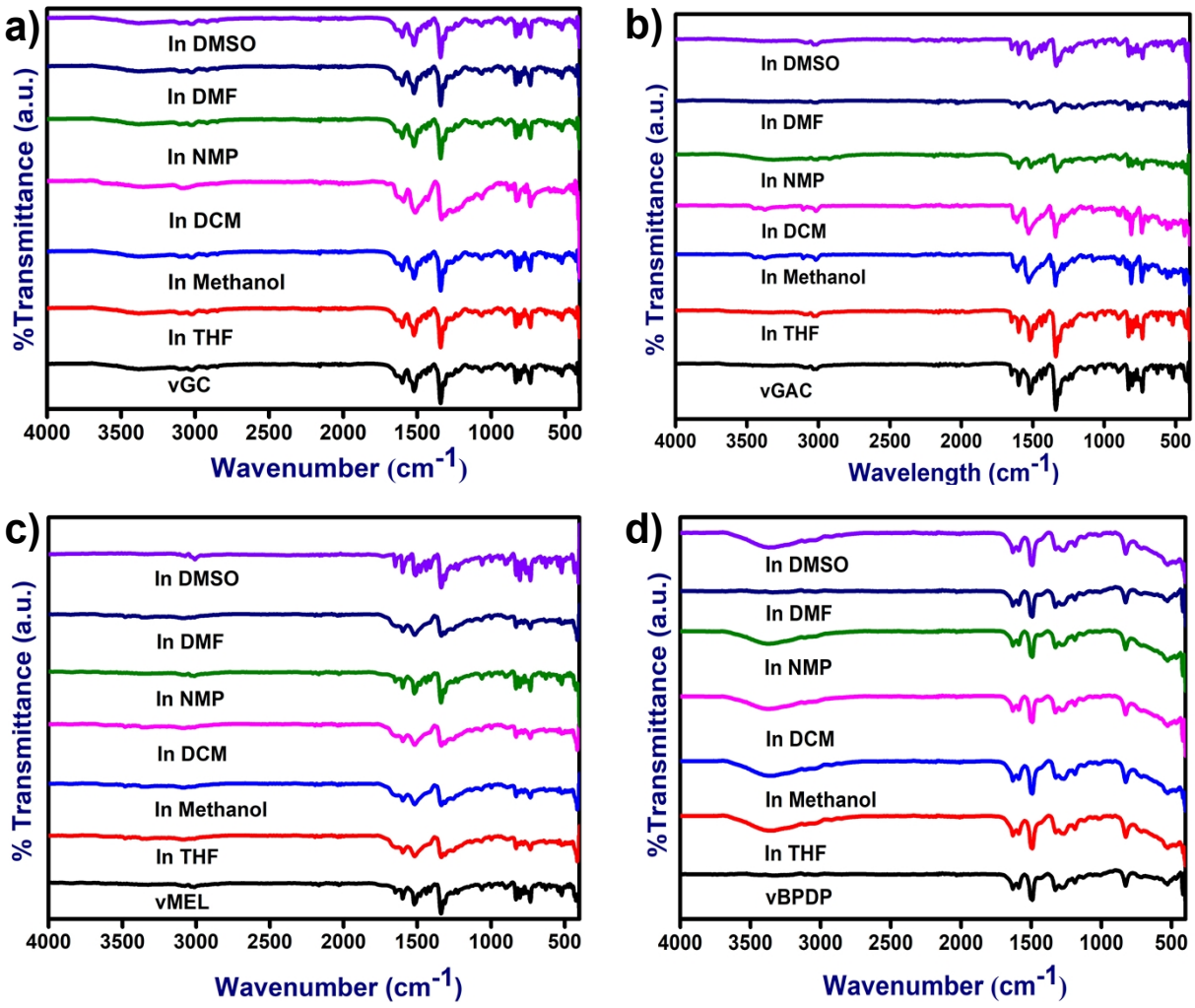

Figure S11: Chemical stability study of vCONs in various polar solvents. We checked vCONs stability in **Methanol, NMP, DMF, DMSO, DCM,** and **THF.** FT-IR spectra of all the solvents treated samples of a) vGC, b) vGAC ,c) vMEL, and d) vBPDP compared with their respective pristine phase.

.

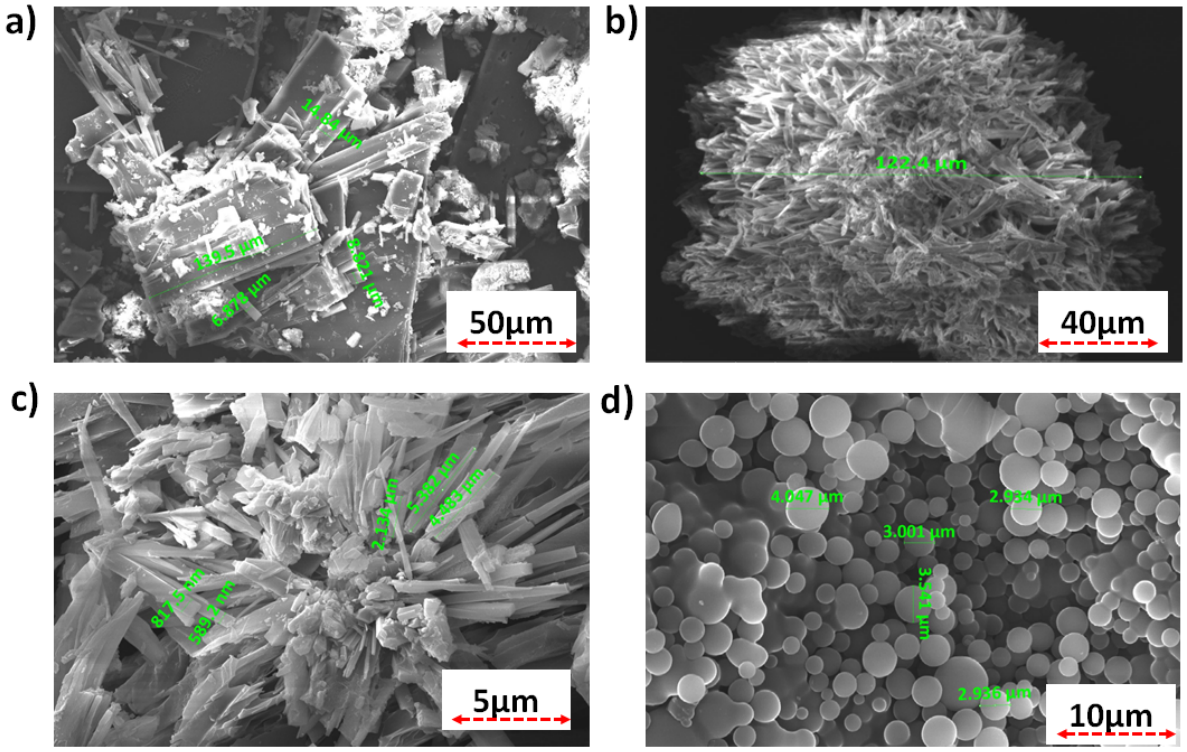

Figure S12: FE-SEM micrographs of a) vGC, b) vGAC, c) vMEL, and d) vBPDP

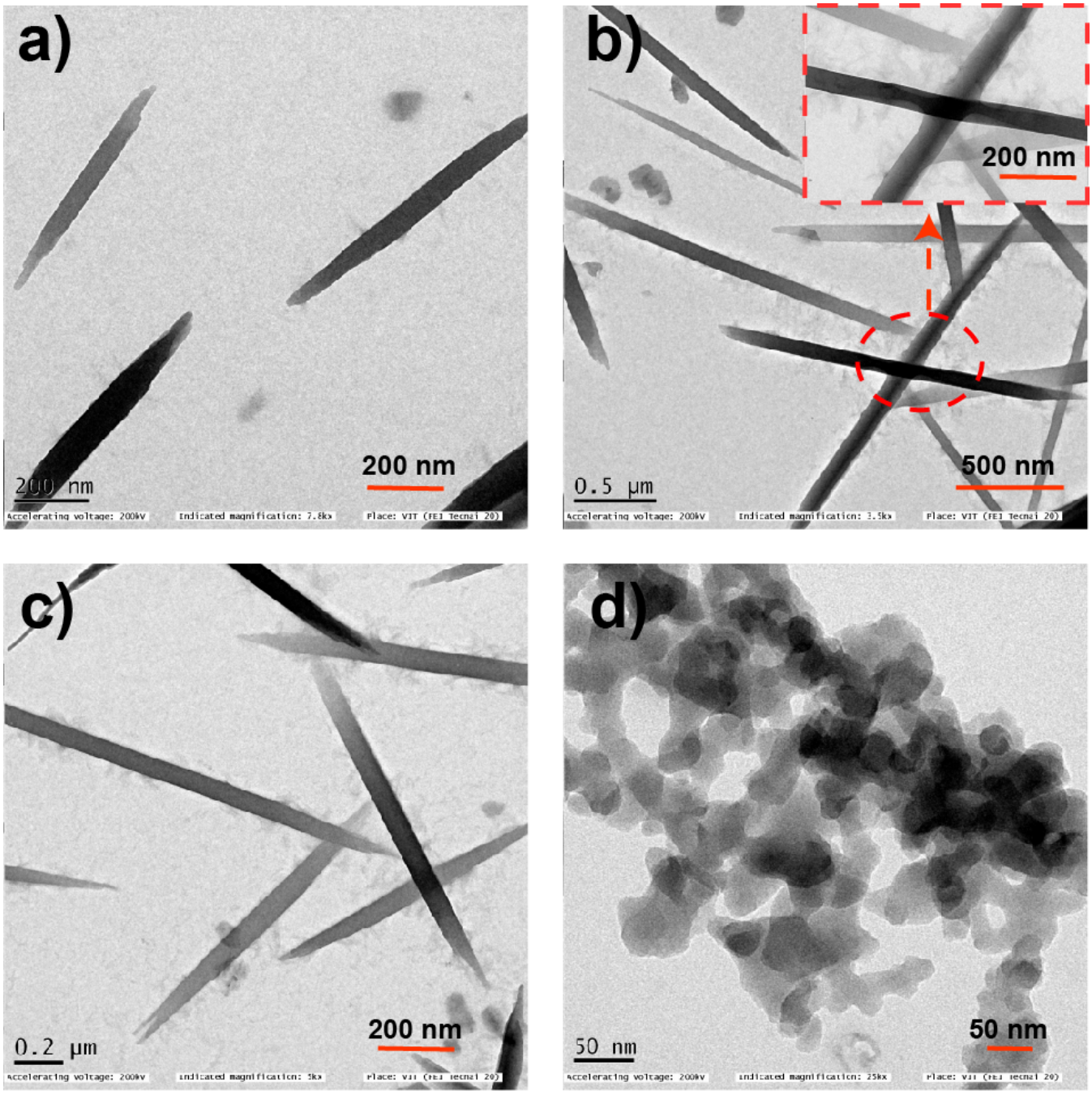

Figure S13: HRTEM images of vCONs, a) vGC, b) vGAC, c) vMEL, and d) vBPDP under solvothermal reaction.

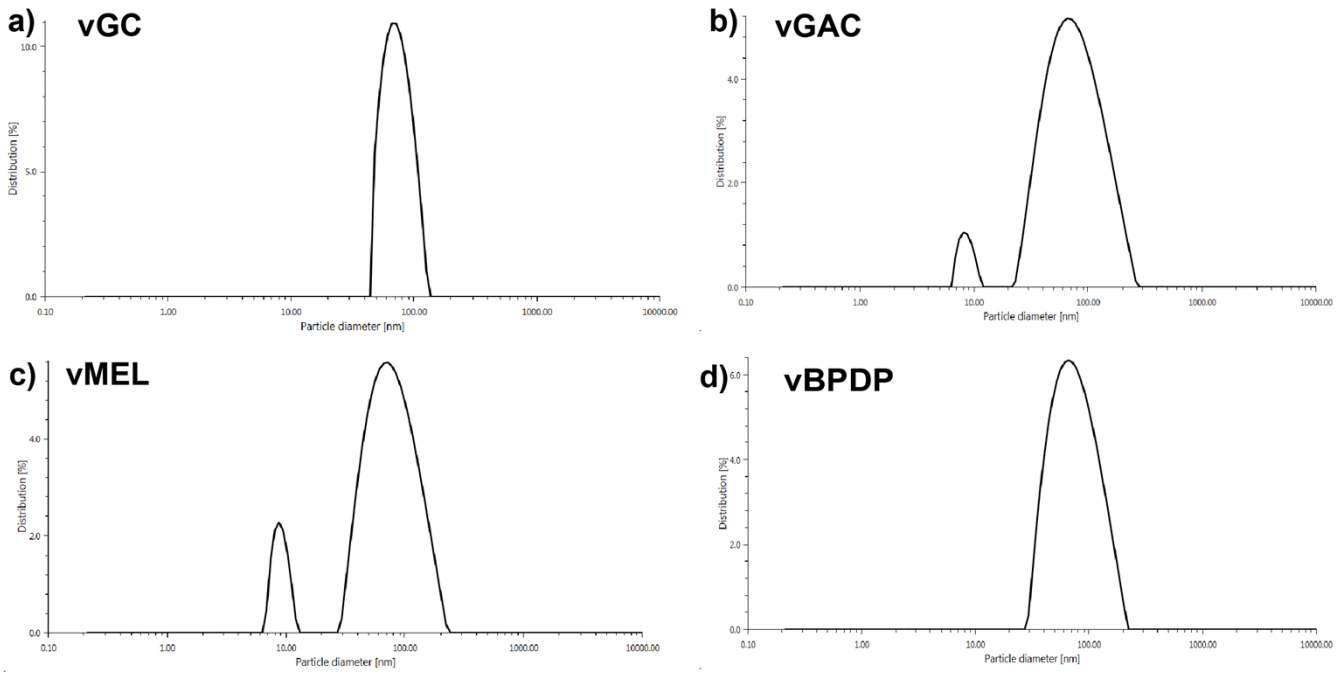

Figure S14: DLS particle size analysis of vCONs, a) vGC, b) vGAC, c) vMEL, and d) vBPDP under solvothermal reaction.

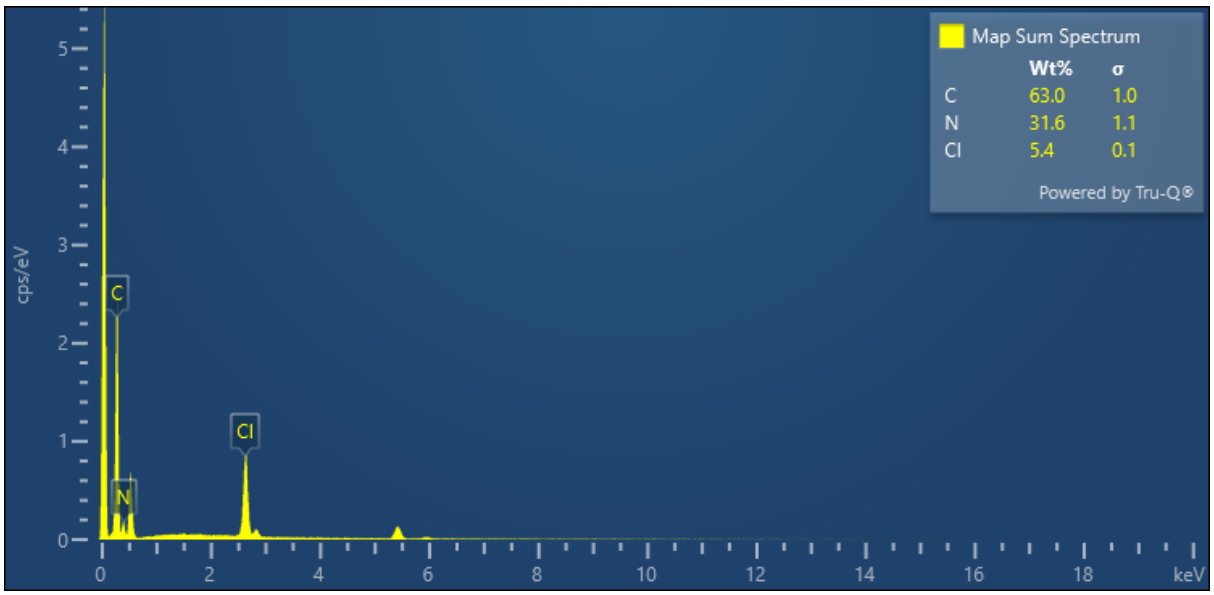

Figure S15: FESEM-EDAX analysis of vGC that contain 68.7% of carbon, 30.5% of nitrogen and 0.7% chlorine.

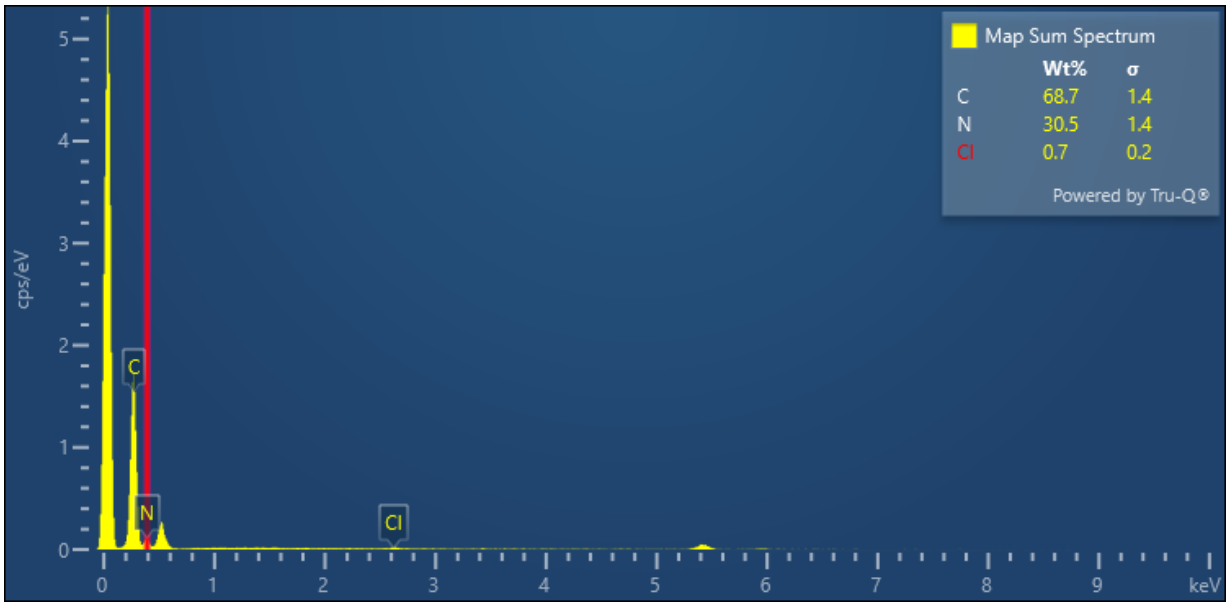

Figure S16: FESEM-EDAX analysis of vGAC showed 63% f carbon, 31.6% nitrogen and 5.4% chlorine.

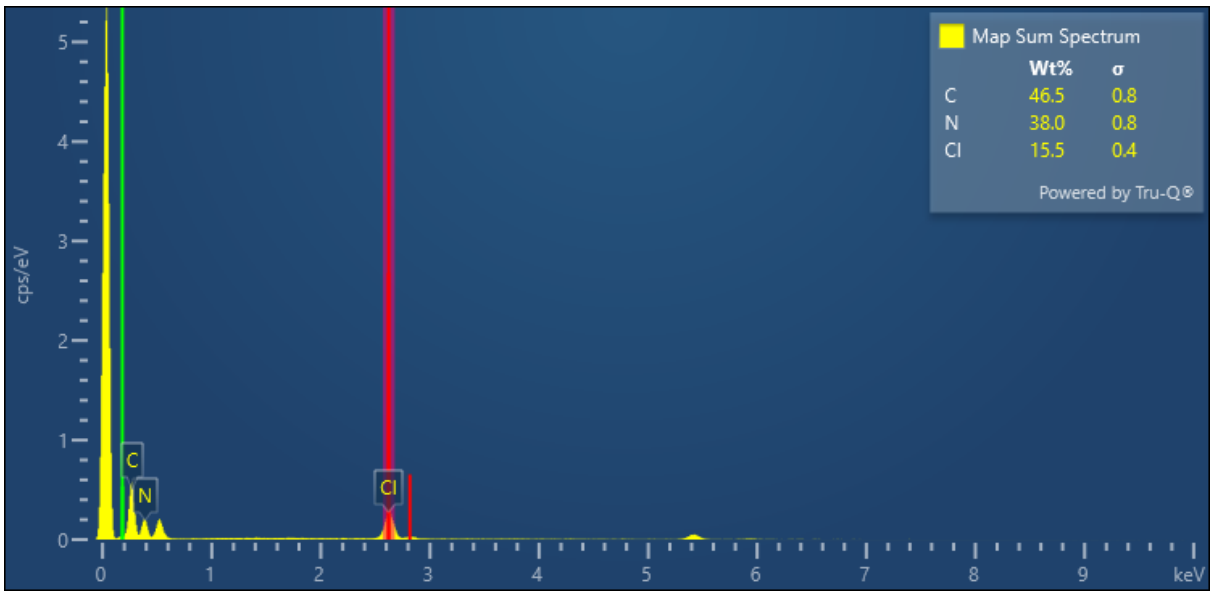

Figure S17: FESEM-EDAX analysis of vMEL showed 46.5% carbon, 38% nitrogen and 15.5% chlorine.

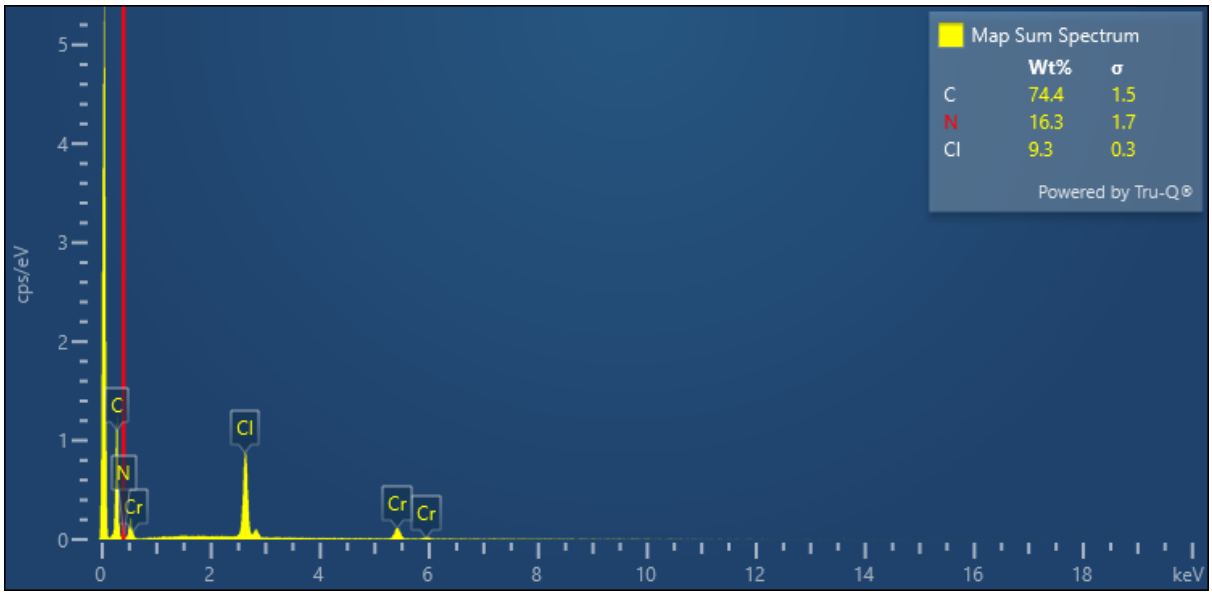

Figure S18: FESEM-EDAX analysis of vBPDP showed 74.4% of carbon, 16.3% nitrogen and 9.3% chlorine.

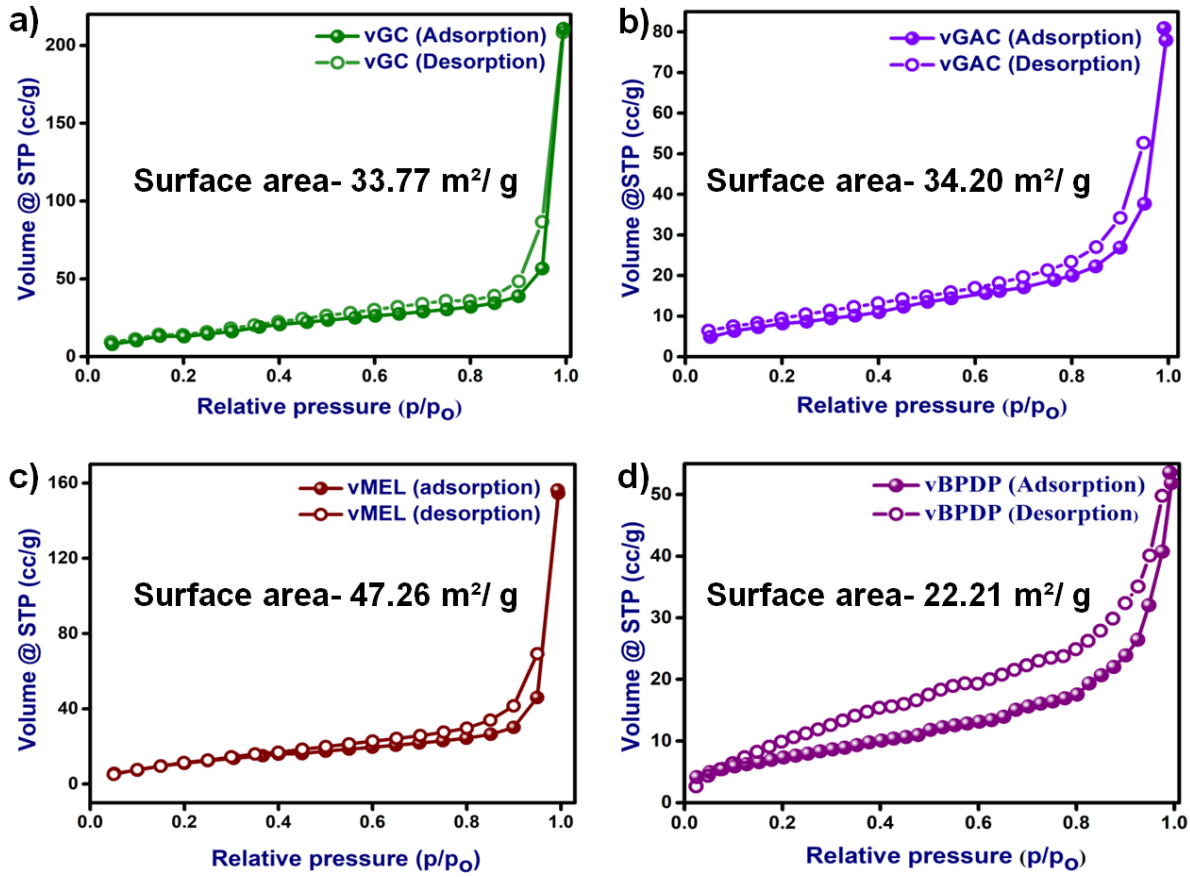

Figure S19: Nitrogen adsorption isotherm and BET surface area analysis of a) vGC, b) vGAC , c) vMEL, and d) vBPDP.

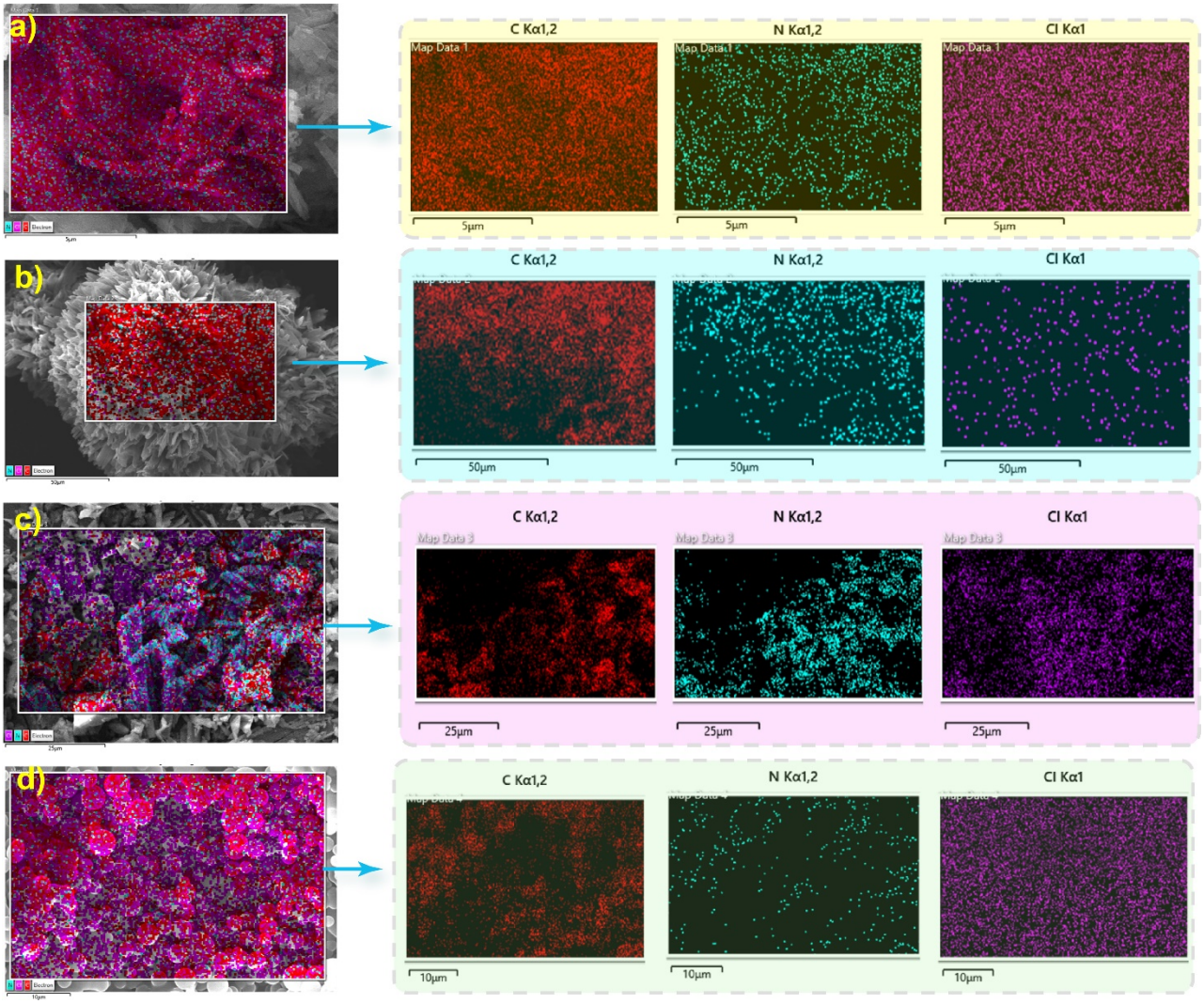

Figure S20: FESEM-EDX elemental mapping of a) vGC, b) vGAC , c) vMEL, and d) vBPDP. All these case mapping showed the homogeneous distribution of C, N and Cl in vCONs structure.

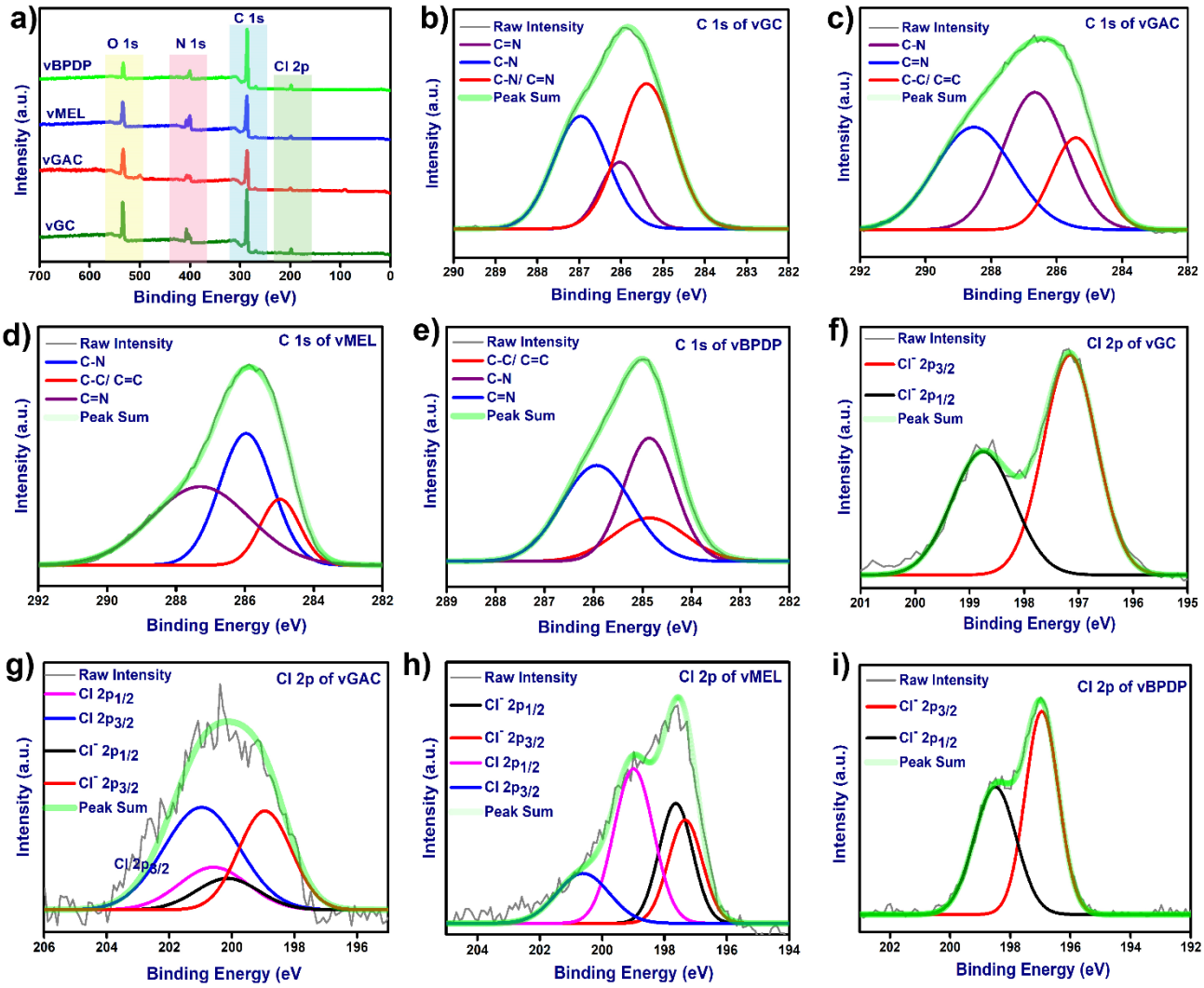

Figure S21: XPS spectra of all vCONs. **a)** Combined survey scan of all vCONs, (**b-e)** represented the C 1s XPS spectra and (**f-i)** showed the Cl 2p XPS spectra of vGC, vGAC, vMEL and vBPDP respectively.

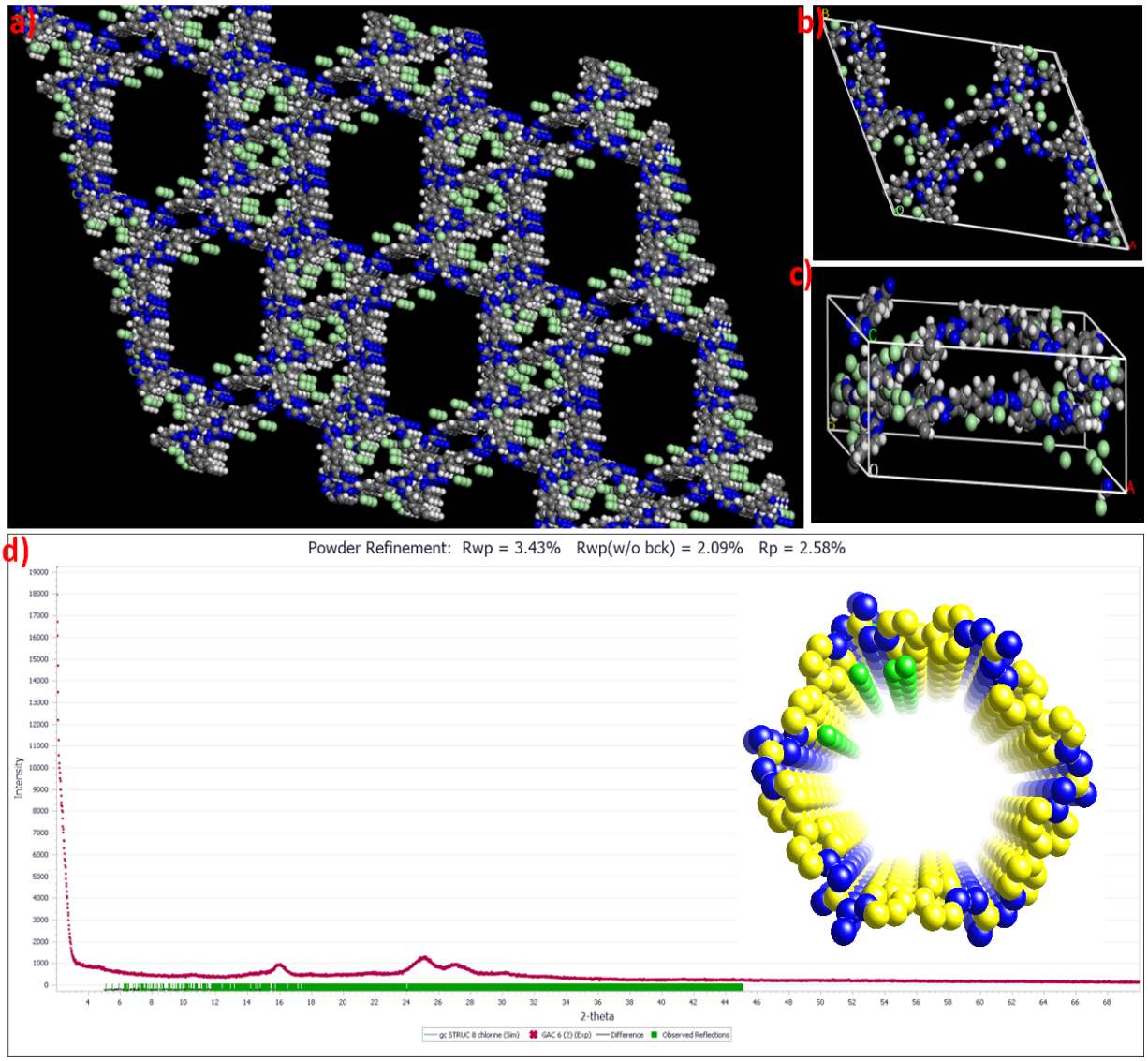

Figure S22: Crystal Structure analysis of vGAC a) extended supercell structure of vGAC, (b-c) representation of the unit cell of vGAC, d) Powley refinement of simulated vGAC structure with the experimental powder pattern (R_{wp} is 3.43%).

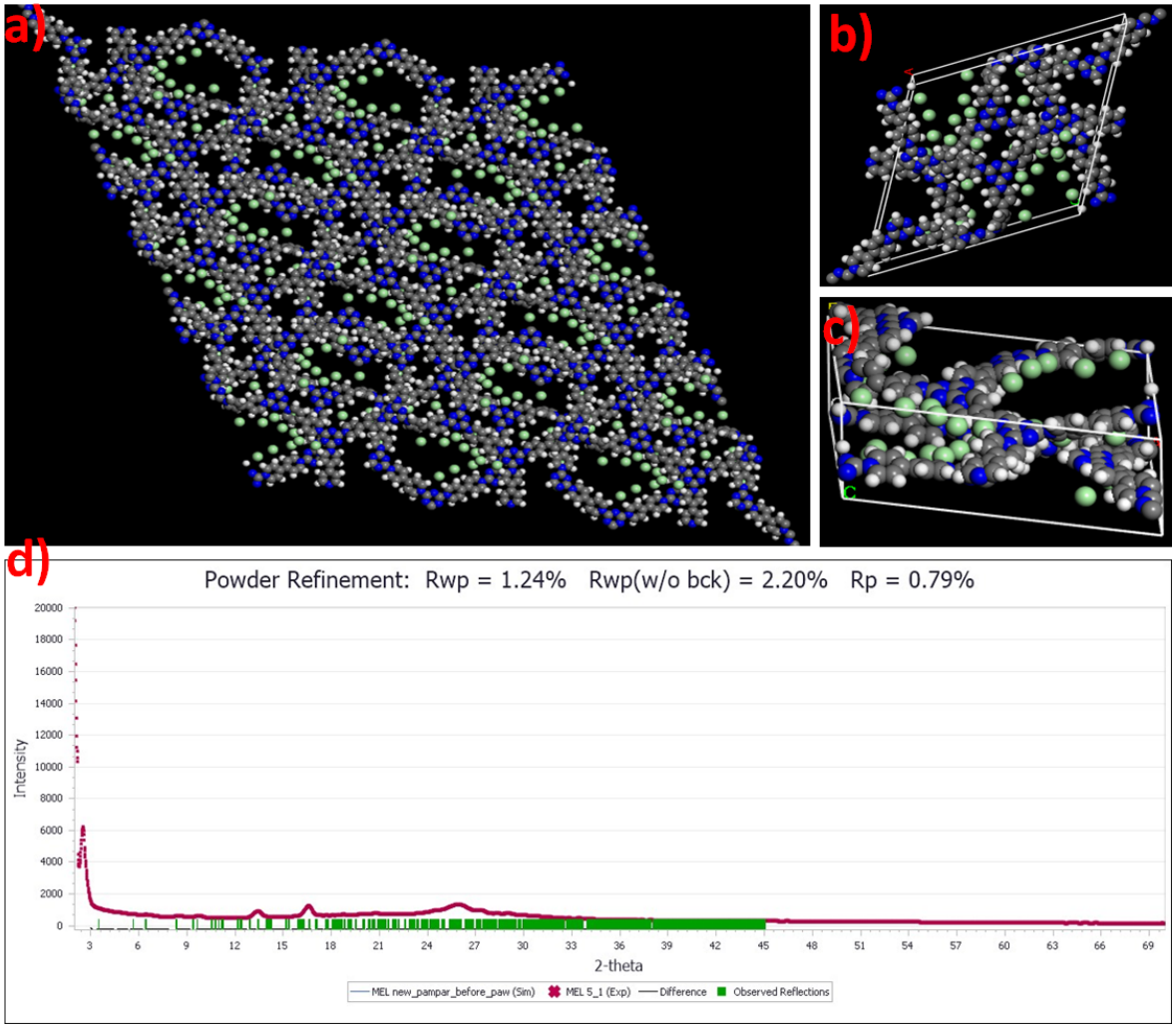

Figure S23: Crystal Structure analysis of vMEL a) extended supercell structure of vMEL b-c) representation of the unit cell structure of vMEL, d) Powley refinement of simulated vMEL structure with the experimental powder pattern (R_{wp} is 1.24%).

S-4: Electrochemical studies of vCONs

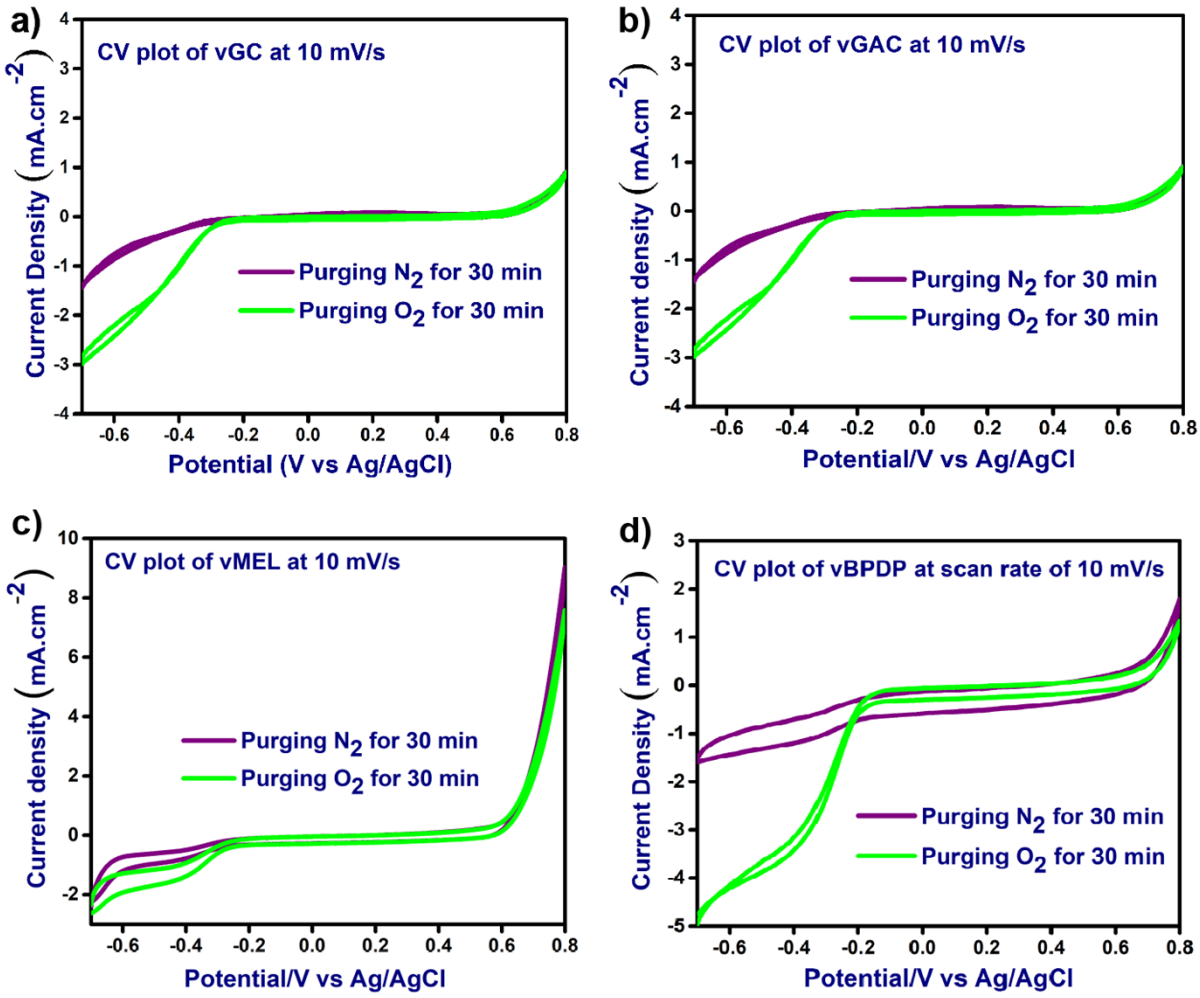

Figure S24: Cyclic voltammetry CV curves of a) vGC, b) vGAC , c) vMEL, and d) vBPDP at 10mV/s

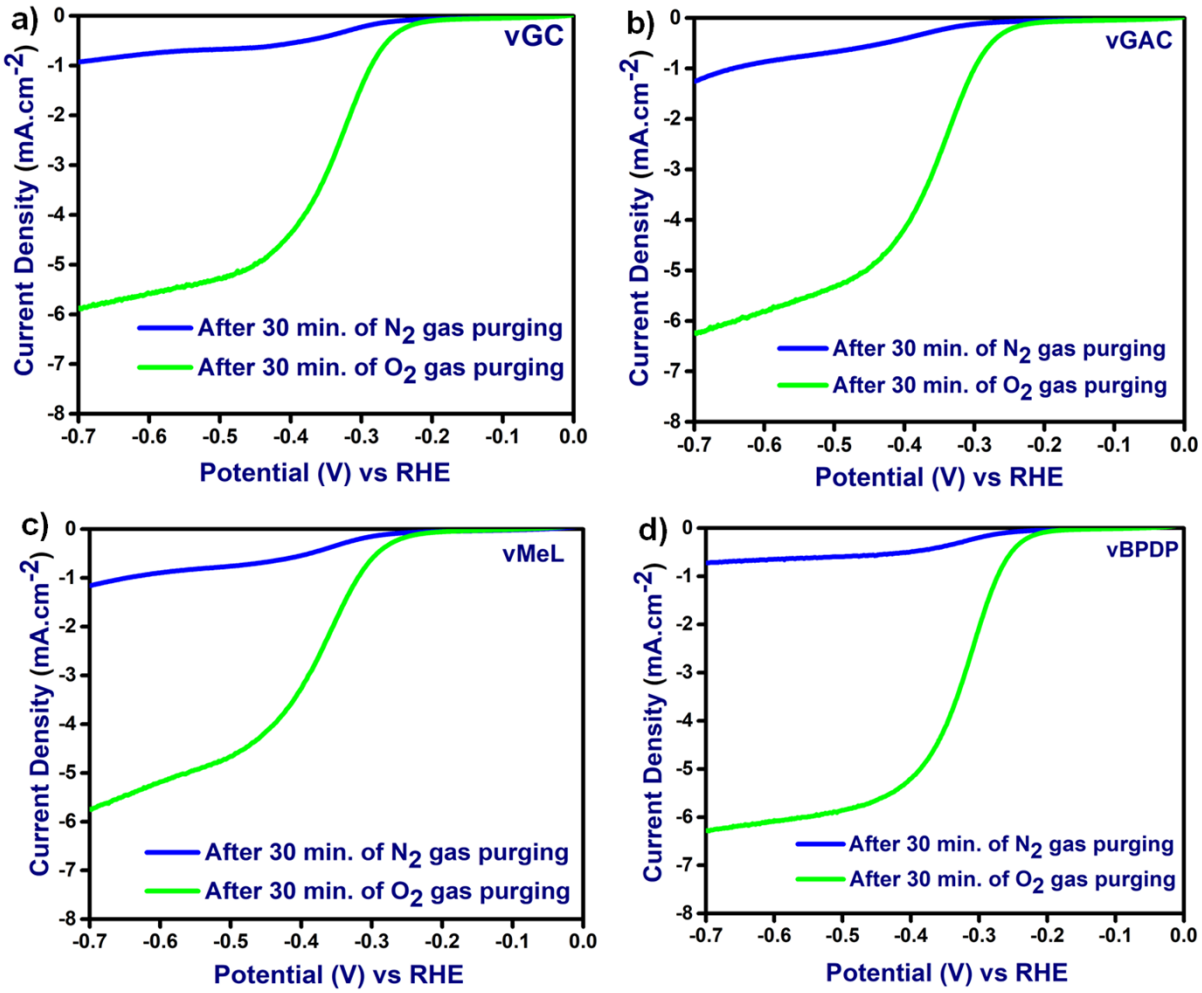

Figure S25: Polarisation curves of a) vGC, b) vGAC , c) vMEL, and d) vBPDP.

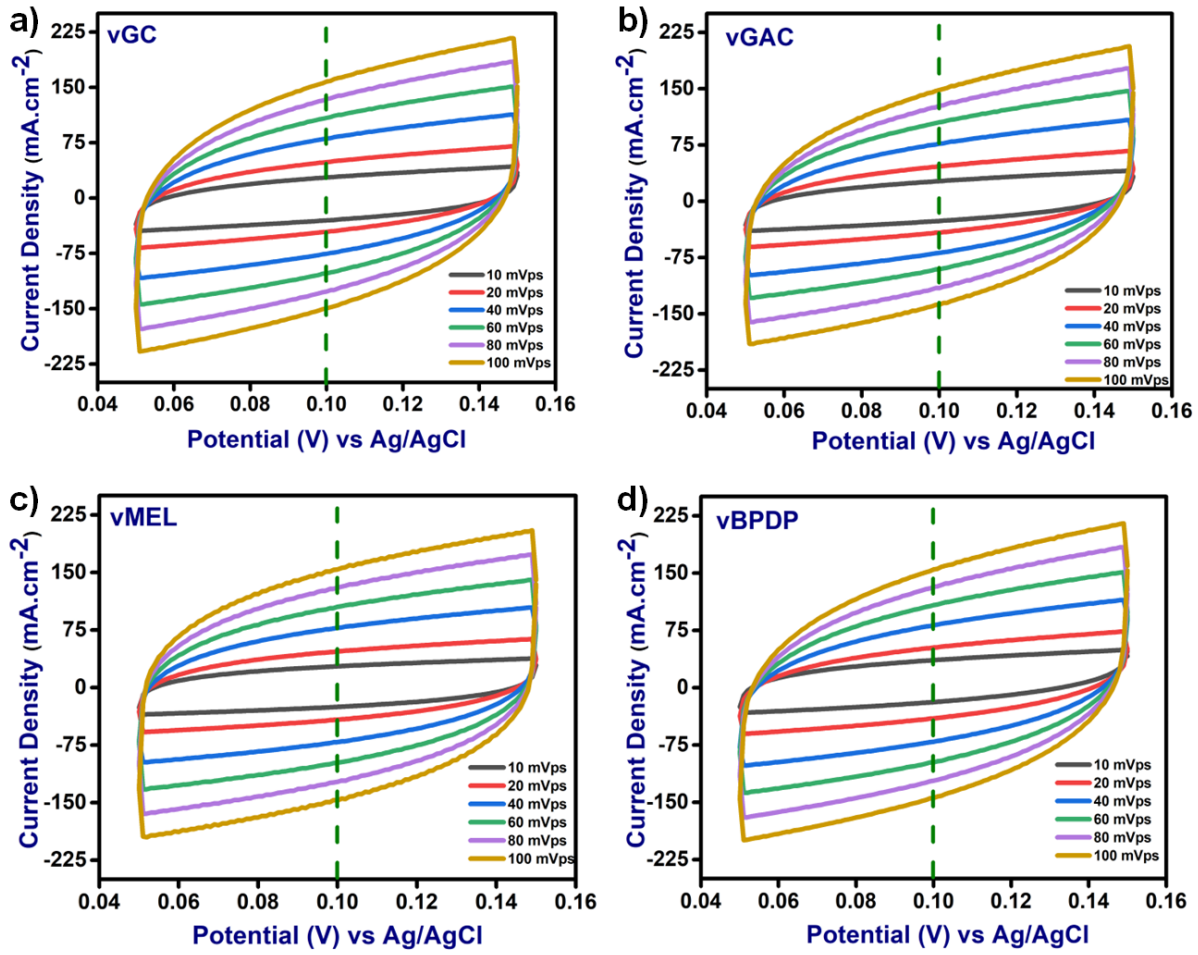

Figure S26: Cyclic voltammetry scans of a) vGC, b) vGAC , c) vMEL, and d) vBPDP at various current densities to determine the electrochemical double layered capacitance and electrochemical active surface area (ECSA).

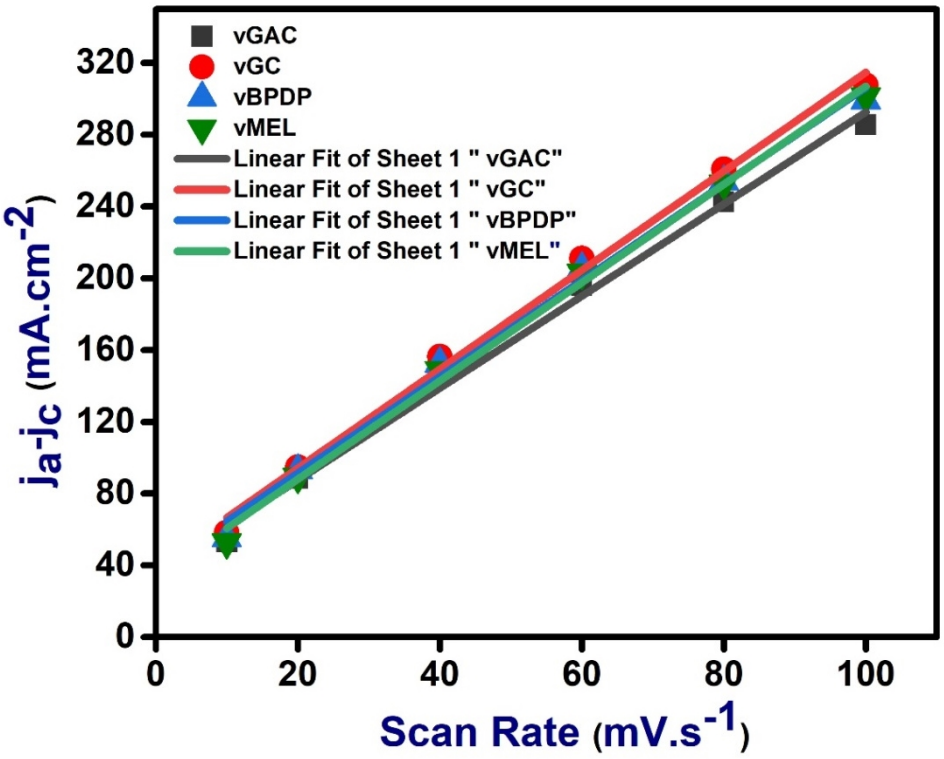

Figure S27: Determination of electrochemical double layered capacitance EDLC and electrochemical active surface area (ECSA).

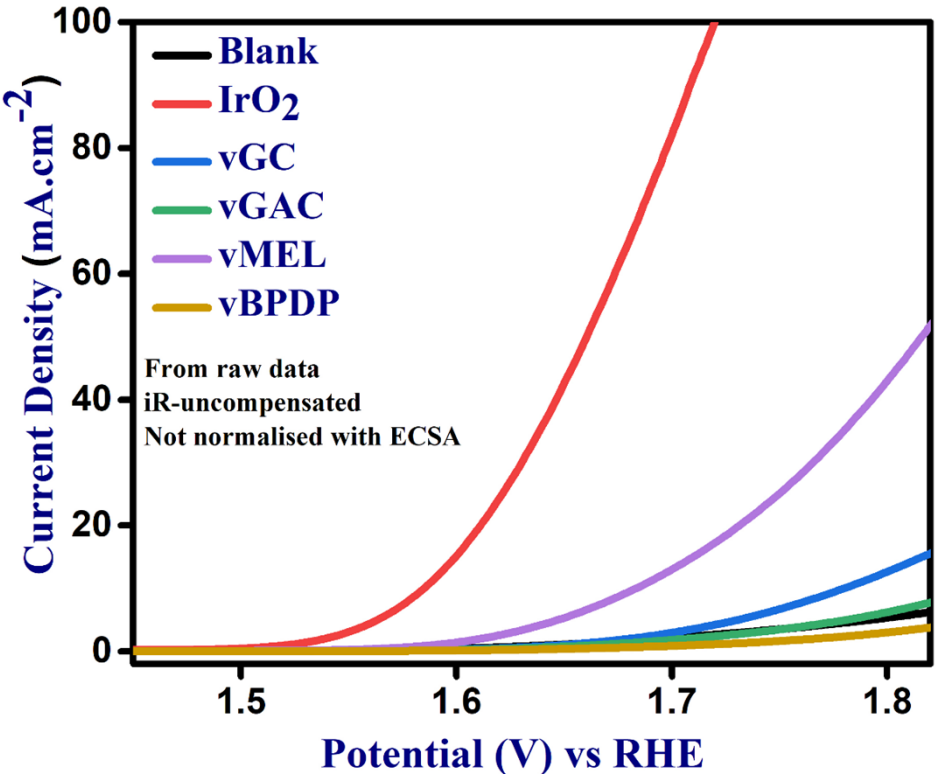

Figure S28: LSV curves in 1.0 M KOH solution of Blank, IrO_2, vGC, vGAC, vMEL and vBPDP at 5 mV s^{-1} with and without iR-correction for OER.

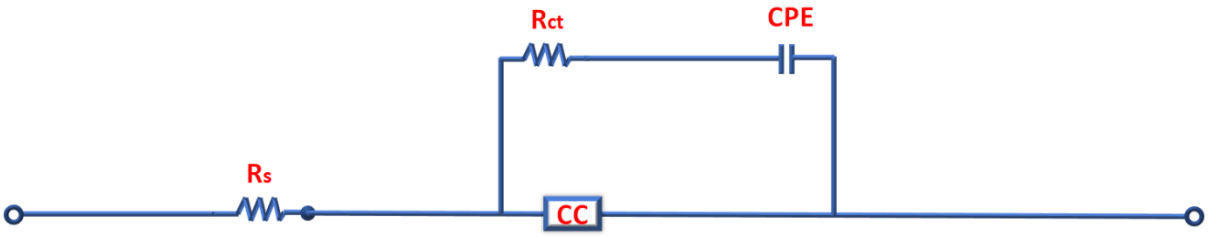

Figure S29: The equivalent circuit used to fit the experimental data of EIS spectra of vCONs (R_s: electrolyte resistance, R_{ct}: charge transfer resistance, CPE: double layer capacity).

S-5: Supplementary Table

Table -S1a: Various synthetic procedure of vGC:

Sl.no	Reactant	Reaction condition	Solvent	Product	Yield
1	GC and L1	120°C, 72 hrs	1,4-dioxane / water (2:1)	vGC-1	40%
2			**Ethanol/ water (4:1)**	**vGC-2**	**63%**
3			Ethanol/ Cl-benzene/ 1,4-dioxane (1:1:1)	vGC-3	30%
4	**same**	**same**	**Mesitylene/ 1,4-dioxane (1:1)**	**vGC-4**	**Not formed**
5			**1,4-dioxane/ ethanol (1:1)**	**vGC-5**	**Not formed**
6			**Ethanol/ mesitylene (1:1)**	**vGC-6**	**Not formed**

Table -S1b: Various synthetic procedure of vGAC

Sl. no	Reactant	Reaction condition	Solvent	Product	Yeild
1	GAC and L1	120°C, 72 hrs	1,4-dioxane / water (2:1)	vGAC-1	70%
2			**Ethanol/ water (4:1)**	**vGAC-2**	**83%**
3			Ethanol/ Cl-benzene/ 1,4-dioxane (1:1:1)	vGAC-3	72%
4	same	same	Mesitylene/ 1,4-dioxane (1:1)	vGAC-4	61%
5			**1,4-dioxane/ ethanol (1:1)**	**vGAC-5**	**Not formed**
6			Ethanol/ mesitylene (1:1)	vGAC-6	22%

Table -S1c: Various synthetic procedure of vMEL.

Sl.no	Reactant	Reaction conditions	Solvent	Product	Yield
1	MEL and L1	120°C, 72 hrs	1,4-dioxane / water (2:1)	vMEL-1	30%
2			**Ethanol/ water (4:1)**	**vMEL-2**	**75%**
3			Ethanol/ Cl-benzene/ 1,4-dioxane (1:1:1)	vMEL-3	45%
4	same		Mesitylene/ 1,4-dioxane (1:1)	vMEL-4	32%
5			**1,4-dioxane/ ethanol (1:1)**	**vMEL-5**	**Not formed**
6			Ethanol/ mesitylene (1:1)	vMEL-6	25%

Table -S1d: Various synthetic procedure of vBPDP

Sl.no	Reactant	Reaction conditions	Solvent	Product	Yield
1	BPDP and L1	120°C, 72 hrs	1,4-dioxane / water (2:1)	vBPDP-1	56%
2			**Ethanol/ water (4:1)**	**vBPDP-2**	**89%**
3			Ethanol/ Cl-benzene/ 1,4-dioxane (1:1:1)	vBPDP-3	85%
4	same		Mesitylene/ 1,4-dioxane (1:1)	vBPDP-4	60%
5			**1,4-dioxane/ ethanol (1:1)**	**vBPDP-5**	**Not formed**
6			**Ethanol/ mesitylene (1:1)**	**vBPDP-6**	**Not formed**

Table S2: Summary of the reported Covalent organic networks/COFs-based materials as bifunctional electrocatalysts for ORR and OER application.

SL No.	Covalent organic networks/COF based materials as bifunctional electrocatalyst	Modification in electrocatalyst	Electro lyte	E_o(V)	$E_{1/2}$(v)	Over pote ntial (mV)	Tafel slope ($mVdec^{-1}$)	Ref.
1.	**vGC**	**Pristine**	**1M KOH**	**0.76**	**0.69**	**339**	**143.5**	**This work**
2.	**vGAC**	**Pristine**	**1M KOH**	**0.79**	**0.71**	**350**	**195.7**	**This work**
3.	**vMEL**	**Pristine**	**1M KOH**	**0.75**	**0.67**	**300**	**109.4**	**This work**
4.	**vBPDP**	**Pristine**	**1M KOH**	**0.80**	**0.72**	**370**	**191.4**	**This work**
5.	Ni/Fe-COF@CNT900	Hybrid of COF based material and carbon nanotube (CNT), anchored with Ni cultures and Fe nanoparticles and pyrolyzed at 900°C	0.1 M KOH	1.00	0.87	320	61	S3
6.	G@POF-Co	Cobalt coordinated porphyrin organic framework hybridized with graphene	0.1 M KOH	-	0.81	-	120	S4
7.	Co@TAPA-PG	Cobalt nanoparticle encapsulated porous organic polymer	0.1 M KOH	0.88	-	410	111	S5
8.	CoNP-PTCOF	Cobalt nanoparticle encapsulated covalent organic framework	0.1M KOH	-	0.85	400	101	S6
9.	RMCOP-PA-900	Nitrogen and Phosphorus dopped covalent organic framework pyrolyzed at 900°C	0.1 M KOH	1.5	0.84	-	66	S7

S-6. References:

1. P. Samanta, P. Chandra, S. Dutta, Aamod V. Desai, S. K. Ghosh, *Chem. sci.* 2018, **9**, 7874-7881.
2. A. F. M. El-Mahdy, C.-H. Kuo, A. Alshehri, C. Young, Y. Yamauchi, J. Kim, S.-W. Kuo, *J. Mat. Chem. A* 2018, **6**, 19532-19541.
3. Q. Xu, J. Qian, D. Luo, G. Liu, Y. Guo, G. Zeng, *Adv. Sustain. Syst.* 2020, **4**, 2000115.
4. B.-Q. Li, S.-Y. Zhang, X. Chen, C.-Y. Chen, Z.-J. Xia, Q. Zhang, *Adv. Funct. Mater.* 2019, **29**, 1901301.
5. A. Singh, D. Samanta, T. K. Maji, *ChemElectroChem* 2019, **6**, 3756-3763.
6. B.-Q. Li, C.-X. Zhao, S. Chen, J.-N. Liu, X. Chen, L. Song, Q. Zhang, *Adv. Mater.*2019, **31**, 1900592.
7. X. Lin, P. Peng, J. Guo, Z. Xiang, *Chem. Eng. J.* 2019, **358**, 427-434.